Available online at www.sciencedirect.com
ScienceDirect
Physica A 387 (2008) 2279–2292
PHYSICA A
www.elsevier.com/locate/physa

Altered phase interactions between spontaneous blood pressure and flow fluctuations in type 2 diabetes mellitus: Nonlinear assessment of cerebral autoregulation

Kun Hu[a,*], C.K. Peng[b], Norden E. Huang[c,d], Zhaohua Wu[e], Lewis A. Lipsitz[a,f], Jerry Cavallerano[g], Vera Novak[a,**]

[a] *Division of Gerontology, Beth Israel Deaconess Medical Center, Harvard Medical School, Boston, MA, United States*
[b] *Division of Interdisciplinary Medicine & Biotechnology and Margret and H.A. Rey Institute for Nonlinear Dynamics in Medicine, Beth Israel Deaconess Medical Center/Harvard Medical School, Boston, MA, United States*
[c] *Research Center for Adaptive Data Analysis, National Central University, Chungli, Taiwan, ROC*
[d] *Division of Mechanics, Research Center for Applied Sciences, Academia Sinica, Taipei, Taiwan, ROC*
[e] *Center for Ocean-Land-Atmosphere Studies, Calverton, MD, United States*
[f] *Hebrew SeniorLife, Boston, MA, United States*
[g] *Beetham Eye Institute, Joslin Diabetes Center, Boston, MA, United States*

Received 21 November 2007
Available online 8 December 2007

Abstract

Cerebral autoregulation is an important mechanism that involves dilatation and constriction in arterioles to maintain relatively stable cerebral blood flow in response to changes of systemic blood pressure. Traditional assessments of autoregulation focus on the changes of cerebral blood flow velocity in response to large blood pressure fluctuations induced by interventions. This approach is not feasible for patients with impaired autoregulation or cardiovascular regulation. Here we propose a newly developed technique—the multimodal pressure-flow (MMPF) analysis, which assesses autoregulation by quantifying nonlinear phase interactions between spontaneous oscillations in blood pressure and flow velocity during resting conditions. We show that cerebral autoregulation in healthy subjects can be characterized by specific phase shifts between spontaneous blood pressure and flow velocity oscillations, and the phase shifts are significantly reduced in diabetic subjects. Smaller phase shifts between oscillations in the two variables indicate more passive dependence of blood flow velocity on blood pressure, thus suggesting impaired cerebral autoregulation. Moreover, the reduction of the phase shifts in diabetes is observed not only in previously-recognized effective region of cerebral autoregulation (<0.1 Hz), but also over the higher frequency range from ∼0.1 to 0.4 Hz. These findings indicate that type 2 diabetes mellitus alters cerebral blood flow regulation over a wide frequency range and that this alteration can be reliably assessed from spontaneous oscillations in blood pressure and blood flow velocity during resting conditions. We also show that the MMPF

Abbreviations: Blood pressure, BP; Blood flow velocity, BFV; Multimodal pressure-flow analysis, MMPF

* Corresponding address: Division of Gerontology, Beth Israel Deaconess Medical Center, Harvard Medical School, 812 Stoneman Bldg, 330 Brookline Avenue, Boston, MA 02115, United States. Tel.: +1 617 667 0346; fax: +1 617 278 0683.

** Corresponding address: Division of Gerontology, Beth Israel Deaconess Medical Center, Harvard Medical School, LMOB Suite 1b, 110 Francis Street, Boston, MA 02115, United States. Tel.: +1 617 632 8680; fax: +1 617 632 8673.

E-mail addresses: khu@bidmc.harvad.edu, khu@bu.edu (K. Hu), vnovak@bidmc.harvard.edu (V. Novak).

0378-4371/$ - see front matter
doi:10.1016/j.physa.2007.11.052

method has better performance than traditional approaches based on Fourier transform, and is more suitable for the quantification of nonlinear phase interactions between nonstationary biological signals such as blood pressure and blood flow.

PACS: 87.15.Ya; 87.19.U-; 87.63.dk; 89.20.-a

Keywords: Nonstationary; Nonlinear phase interaction; Instantaneous phase shift; Cerebral autoregulation; Cerebral blood flow velocity; Multimodal pressure-flow analysis

1. Introduction

Cerebral autoregulation regulates cerebral blood flow by adjusting the small-vessel resistances in response to beat-to-beat blood pressure (BP) fluctuations [1,2]. It can be damaged by small-vessel ischaemic cerebrovascular disease associated with diabetes mellitus, stroke [3–5] and brain injury [6,7]. Impaired cerebral autoregulation leads to dependence of blood flow on blood pressure, which may affect blood supply to brain when peripheral blood pressure is reduced under physiological and pathological conditions. Therefore, reliable evaluation of cerebral autoregulation is important for diagnosis and clinical assessment of cerebrovascular disease.

Conventional approaches model autoregulation with blood pressure as input and blood flow as output [8,9]. A transfer function is typically used to explore the relationship between blood pressure (BP) and blood flow velocity (BFV) by calculating gain and phase shift between the BP and BFV power spectra [2,8,10–16]. In this approach, it is presumed that signals are stationary, and are composed of superimposed sinusoidal oscillations of constant amplitude and period at a predetermined frequency range. However, blood pressure and blood flow velocity signals recorded in clinical settings are often nonstationary and are modulated by nonlinearly interacting processes at multiple time-scales corresponding to the beat-to-beat systolic pressure, respiration, spontaneous BP fluctuations, and those induced by interventions. Therefore, reliable measures of the nonlinear BP–BFV relationship without preassuming oscillation frequencies and waveform shapes are needed.

To overcome problems related to nonstationarity and nonlinearity, a novel computational method called multimodal pressure-flow (MMPF) analysis was recently developed to study the blood pressure-flow relationship during the Valsalva manoeuvre (See Section 2.4) [17]. The MMPF method can reliably extract BP and BFV oscillations induced by the intervention (i.e., sudden reduction followed by an increase in BP and BFV), and enables evaluation of cerebral autoregulation based on instantaneous phase analysis of BP and BFV oscillations. Applying this technique, a characteristic phase lag between BFV and BP oscillations was found in healthy subjects and this phase lag was reduced in patients with hypertension and stroke that are associated with impaired autoregulation [17]. These findings suggest that BP–BFV phase shift could serve as an index of cerebral autoregulation. However, intervention procedures, such as the Valsalva manoeuvre, introduce large intracranial pressure fluctuations and require patients' cooperation, and such procedures are limited for clinical evaluation of autoregulation.

We hypothesize that the dynamics of cerebral autoregulation can be evaluated from spontaneous BP–BFV fluctuations during supine rest. This hypothesis is motivated by the observation that blood pressure and blood flow velocity can be entrained by respiration or other external perturbation [18,19], and exhibit spontaneous oscillations over a wide frequency ranges (0.05–0.4 Hz) even during resting conditions [14,15,20–22]. Therefore, similarly to BP and BFV oscillations introduced by the Valsalva manoeuvre, there would be phase shifts between spontaneous BP and BFV oscillations during baseline condition and BP–BFV phase shifts would be reduced in subjects with impaired autoregulation.

In order to better quantify the nonlinear BP–BFV relationship, here we propose an improved MMPF method, which uses the Ensemble Empirical Mode Decomposition [23] to extract spontaneous BFV and BP oscillations during resting conditions and uses Hilbert transform to measure continuously instantaneous phase shifts between spontaneous BFV and BP oscillations (see details in Section 2.4). To test our hypothesis, we apply the improved MMPF to BP and BFV data collected in 20 healthy subjects and 20 subjects with type 2 diabetes mellitus during supine resting conditions. Diabetes is associated with microvascular disease that affects vasomotion and vascular reactivity [24, 25]. Evaluations of BFV responses to hypercapnia and head-up tilt have demonstrated that cerebrovascular reserve and endothelium-dependent vasodilation may be compromised in diabetes [26,27]. We expect that diabetes alters the cerebral autoregulation and thus, BP–BFV phase shifts are reduced in subjects with type 2 diabetes mellitus compared to healthy subjects during supine resting conditions.

Table 1
Demographic characteristics for control and diabetes groups

Group	Control	Diabetes	P
Age (yrs)	55.2 ± 2.6	61.0 ± 1.6	NS
Gender (M, F)	12, 8	11, 9	NS
Race (White, Asian, African American)	18, 1, 1	16, 1,3	NS
Body mass index (kg/m^2)	25.4 ± 0.8	27.9 ± 1.1	NS
Hemoglobin A1C (%)	5.36 ± 0.11	7.30 ± 0.22	<0.0001
Glucose (mg/dL)	79.9 ± 2.6	138.9 ± 16.4	0.004
Total cholesterol (mg/dL)	212.8 ± 10.4	196.8 ± 10.2	NS
Dominant oscillation frequency (Hz)	0.16 ± 0.02	0.25 ± 0.01	0.0001
Respiratory frequency (Hz)	0.20 ± 0.01	0.26 ± 0.01	0.0006
Baseline CO_2 (mm Hg)	38.3 ± 1.2	35.2 ± 0.2	0.03
Diabetes duration (yrs)		11.8 ± 2.5	
Hypertension	0	6	
Retinopathy	0	6	
Orthostatic hypotension (yes)	0	2	
Cardiac-vagal impairment (yes)	0	10	
Baseline heart rate (bpm)	63.3 ± 2.2	69.3 ± 2.4	NS
Systolic blood pressure (mm Hg)	121.8 ± 3.4	131.6 ± 3.8	NS
Diastolic blood pressure (mm Hg)	70.9 ± 2.1	69.5 ± 1.8	NS
Mean blood pressure (mm Hg)	90.2 ± 2.1	89.2 ± 2.1	NS

Data are presented as mean±SE. P values indicated between group comparisons.

2. Methods

2.1. Subjects

The control group consisted of 12 men and eight women who were normotensive, had normal hemoglobin A1C levels and were not treated for any systemic disease. The diabetes group consisted of 11 men and nine women with type 2 diabetes mellitus (duration 11.8 ± 2.5 years; mean $\pm$ SE). All subjects did not have a history of strokes, clinically important cardiac disease, arrhythmias, significant nephropathy, kidney or liver transplant, renal or congestive heart failure, uncontrolled hypertension, carotid artery stenosis $>50\%$ by medical history and MR angiography, and neurological or other systemic disorders.

Diabetic retinopathy was diagnosed in six diabetic patients with the Joslin Vision Network video-digital retinal imaging system that uses a nonmydriatic retinal fundus camera with low light level imaging without pupil dilatation [28] and has been validated against clinical examination and standard retinal imaging [29]. Two diabetic subjects had autonomic dysfunction with orthostatic hypotension and eight diabetes subjects also had cardiac-vagal impairment. Diabetic subjects were treated with insulin (4), oral glucose-control agents (9) or diet (7). For six hypertensive diabetic subjects, antihypertensive medications were discontinued for three days before the study.

The study was performed in the Syncope and Falls in the Elderly (SAFE) Laboratory at the Beth Israel Deaconess Medical Center (BIDMC). All subjects were recruited consecutively and provided informed consent that was approved by the Institutional Review Boards at the BIDMC and the Joslin Diabetes Center. All subjects were screened with a medical history, physical examination, standard battery of autonomic tests [30] and routine blood and urine chemistries. Demographic and clinical characteristics are summarized in Table 1.

2.2. Data acquisition

The experiments were done in the morning or >2 h after the last meal. Subjects were resting comfortably in supine position in a quiet environment for 20 min during instrumentation for the study. Then data were collected for at least 5 min during the baseline resting conditions when subjects were awake, breathing regularly at their normal respiratory frequency. The electrocardiogram was measured from a modified standard lead II or III using a Spacelab Monitor (SpaceLab Medical Inc., Issaquah, WA). Beat-to-beat blood pressure was recorded with a Finapres device (Ohmeda Monitoring Systems, Englewood CO) from a finger that was kept in a constant temperature. Cerebral blood flow velocity was measured from left and right middle cerebral arteries using transcranial Doppler ultrasonography

system (MultiDop X4, DWL Neuroscan Inc, Sterling, VA). Data was continuously recorded at a sampling frequency of 500 Hz and was resampled to 50 Hz for data analysis.

2.3. Statistical analysis

Descriptive statistics were used to summarize data. We used one-way analysis of variance for between-group comparisons of autoregulation measures and other parameters that may affect autoregulation including age, body mass index, baseline heart rate, BP, BFV, cerebrovascular resistance, respiration frequency and CO_2. Multivariate analysis of variance (MANOVA) with sides (left vs. right middle cerebral artery) as repeated measures was also performed to explore the effects of type 2 diabetes on the cerebral autoregulation assessed by the phase relationship between BP and BFV (JMP-5.0 SAS Institute, Cary, NC). In MANOVA, the BP–BFV phase shifts were adjusted using linear fitting to account for possible effects of the frequency of dominant oscillation (from ∼0.1 to 0.4 Hz) (see Table 1). The adjustment was performed using a linear regression model of phase shift as a function of mean dominant frequency. For each subject, residual values after detrending were added to the mean phase shift to obtain the frequency-adjusted phase shift.

2.4. Multimodal pressure-flow (MMPF) analysis

To quantify the dependency between cerebral blood flow and systemic pressure, we developed MMPF computational method that was recently applied to study the BP–BFV relationship during the Valsalva manoeuvre [17]. The MMPF method includes two major steps: (1) decompose each signal (BP and BFV) into multiple empirical modes; and (2) apply phase analysis to chosen BP oscillations and corresponding BFV oscillations in certain empirical modes.

2.4.1. Signal decomposition

The original MMPF applies the empirical mode decomposition algorithm to decompose complex BP and BFV signals into multiple empirical modes (called intrinsic mode functions) with each mode representing a frequency–amplitude modulation in a narrow band that can be related to a specific physiological process [31]. For a time series $x(t)$ with at least two extremes, the decomposition uses a sifting procedure to extract mode functions one by one from a finest scale to the largest scale,

$$\begin{aligned} x(t) &= s_1(t) + r_1(t) \\ &= s_1(t) + s_2(t) + r_2(t) \\ &\vdots \\ &= s_1(t) + s_2(t) + \cdots + s_n(t) \end{aligned} \tag{1}$$

where $s_k(t)$ is the kth mode function and $r_k(t)$ is the residual after extracting the first k mode functions. Briefly, the extraction of the kth mode function includes the following steps:

(i) Initialize $h_0(t) = h_{i-1}(t) = r_{k-1}(t)$ (if $k = 1$, $h_0(t) = x(t)$), where $i = 1$;
(ii) Extract local minima/maxima of $h_{i-1}(t)$ (if the total number of minima and maxima is less than 2, $s_k(t) = h_{i-1}(t)$ and stop the whole decomposition process);
(iii) Obtain upper envelope (from maxima) and lower envelope (from minima) functions $p(t)$ and $v(t)$ using cubic spline fittings to interpolate local minima and maxima of $h_{i-1}(t)$, respectively;
(iv) Calculate the $h_i(t) = h_{i-1}(t) - (p(t) + v(t))/2$;
(v) Calculate the variance (VA) of $\frac{p(t)+v(t)}{2h_{i-1}(t)}$;
(vi) If the VA is small enough (less than a chosen threshold $\mathrm{VA}_{\max}$, typically between 0.2 and 0.3) [31], the kth mode function is assigned as $s_k(t) = h_i(t)$ and $r_k(t) = r_{k-1}(t) - s_k(t)$; Otherwise repeat steps (ii)–(v) for $i + 1$ until $\mathrm{VA} < \mathrm{VA}_{\max}$.

The above procedure is repeated for $k+1$ to obtain different mode functions at different scales until there are fewer than two minima or maxima in a residual $r_k(t)$ which will be assigned as the last mode function (see the step (ii) above).

A limitation of the empirical mode decomposition in the application for nonstationary biological signals is the "mode mixing" problem; i.e., for signals with intermittent oscillations, a mode obtained from the empirical mode

decomposition could comprise of oscillations with different wavelengths at various temporal locations [32]. In this study, in order to extract the spontaneous oscillations in BP and BFV during baseline conditions, we used an improved decomposition algorithm, namely the Ensemble Empirical Mode Decomposition [23]. This method consists of an ensemble of the empirical mode decompositions of data with added white noise and treats the resultant means of the corresponding intrinsic mode functions from different decompositions as the final result. The new decomposition approach overcomes this limitation and ensures the decompositions to compass the range of possible solutions in the sifting process and to collate the signals of different scale in the proper mode function naturally. Shortly, for a time series $x(t)$, the new decomposition includes the following steps:

(i) Generate a new signal $y(t)$ from the original time series $x(t)$ by superposing to $x(t)$ randomly generated white noise with amplitude equal to 10% of the standard deviation of $x(t)$;
(ii) Perform the empirical mode decomposition on $y(t)$ to obtain intrinsic mode functions;
(iii) Repeat steps (i)–(ii) m times with different white noise to obtain an ensemble of intrinsic mode functions $\{s_k^1(t), k = 1, 2 \ldots, n\}, \{s_k^2(t), k = 1, 2 \ldots, n\}, \ldots, \{s_k^m(t), k = 1, 2 \ldots, n\}$;
(iv) Calculate the average of intrinsic mode functions $\{s_k(t), k = 1, 2 \ldots, n\}$, where $s_k^{(t)} = \frac{1}{m} \sum_{i=1}^{m} s_k^i(t)$.

The last two steps are to reduce noise level and to ensure that the obtained mode functions reflect the true oscillations in the original time series $x(t)$. In this study, we repeated decomposition $m = 100$ times so that the noise level is approximately less than 1%.

The intrinsic modes for BP and BFV signals were obtained using decomposition procedure described above. Then BP and BFV relationship was assessed from spontaneous oscillations in certain intrinsic mode function(s) of BP and BFV signals. Statistically, evaluating several cycles of spontaneous oscillations corresponding to the same physiological functions provides better reliability and reproducibility of the results. Thus, dominant and continuous oscillations in BP and BFV in specific modes can provide a better estimation of BP–BFV phase relationship (Fig. 1). In this study, oscillations in the range of ∼0.01–0.6 Hz were selected for the assessment of autoregulation. We also analysed the oscillations in two frequency regions separately (<0.1 Hz and ∼0.1–0.4 Hz).

2.4.2. Phase analysis

To quantify BP–BFV phase relationship, we applied the Hilbert transform to the extracted BP and BFV oscillations to calculate their instantaneous phases [33]. For a time series $s(t)$, its Hilbert transform is defined as

$$\tilde{s}(t) = \frac{1}{\pi} P \int \frac{s(t')}{t - t'} \mathrm{d}t' \tag{2}$$

where P denotes the Cauchy principal value. Hilbert transform has an apparent physical meaning in Fourier space: for any positive (negative) frequency f, the Fourier component of the Hilbert transform $\tilde{s}(t)$ at this frequency f can be obtained from the Fourier component of the original signal $s(t)$ at the same frequency f after a 90 deg clockwise (anticlockwise) rotation in the complex plane; e.g., if the original signal is $\cos(\omega t)$, its Hilbert transform will become $\cos(\omega t - 90 \text{ deg}) = \sin(\omega t)$. For any signal $s(t)$, the corresponding analytical signal can be constructed using its Hilbert transform and the original signal:

$$S(t) \equiv s(t) + i\tilde{s}(t) = A(t)\mathrm{e}^{\mathrm{i}\varphi(t)} \tag{3}$$

where $A(t)$ and $\varphi(t)$ are the instantaneous amplitude and instantaneous phase of $s(t)$, respectively. To obtain phase values of discrete time series $s(i)$, we implemented the discrete Hilbert transform [34] by doing the convolution of $s(i)$ and $h(i)$, i.e., $\tilde{s}(i) = s(i) * h(i)$, where

$$h(i) = \begin{cases} 0 & i \text{ even} \\ 2/(i\pi) & i \text{ odd.} \end{cases} \tag{4}$$

The convolution was fulfilled by performing discrete Fourier transformation on $s(i)$ and $h(i)$, and inverse discrete Fourier transformation on the product of the two obtained Fourier transforms [34].

Unlike the Fourier transform, the Hilbert transform method does not assume that signals are composed of superimposed sinusoidal oscillations of constant amplitude and frequency [33]. Rather, it provides instantaneous phase $\varphi(t)$ and local amplitude $A(t)$ of an oscillation. Real-world biological fluctuations, such as BP and BFV, are

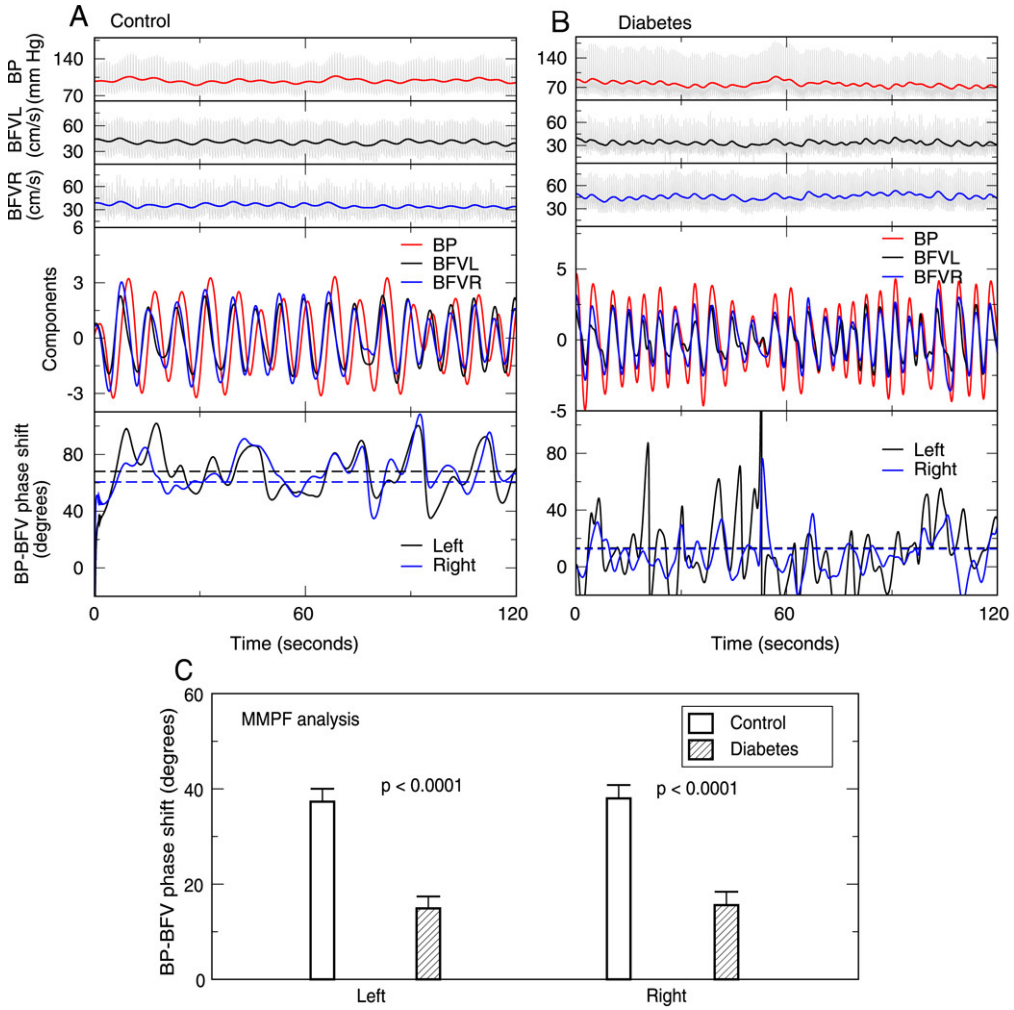

Fig. 1. Dominant spontaneous oscillations of blood pressure (BP) and cerebral blood flow velocity (BFV) in (A) a 72-year-old healthy control woman and (B) a 68-year-old man with type 2 diabetes mellitus during supine baseline. BP, left and right BFVs (Panels 1–3 in A and B) were decomposed into different modes using ensemble empirical mode decomposition algorithm, each mode corresponding to fluctuations at a different time scale. BP and BFV fluctuations exhibit continuous and dominant oscillations at the frequency from ∼0.07 to 0.4 Hz (Panel 4 in A and B). The dominant oscillations were extracted and used for the assessment of BP–BFV phase relationship. Instantaneous phases of BP and BFV oscillations (solid lines in the bottom panels of A and B) were obtained using the Hilbert transform. For each subject, the mean BP–BFV phase shift (horizontal dashed lines in bottom panels of A and B) was obtained as the average of instantaneous BP–BFV phase shifts for all cycles of dominant oscillations. (C) Phase shifts between spontaneous dominant oscillations of BP and BFV were much smaller in diabetes group than in healthy control group ($p < 0.0001$). The group averages of BP–BFV phase shifts for control and diabetes are shown in columns with error bars as the standard errors. There was no significant difference in phase shifts between left and right blood flow velocities in both control and diabetes groups.

not stationary and are better described by analytical methods that can quantify variations of amplitude and frequency. For this reason, the Hilbert transform provides a more informative and accurate tool to examine nonlinear relationship between nonstationary signals [33].

The instantaneous BP and BFV phases were calculated on a sample-by-sample basis. The BP–BFV phase shift for each subject was calculated as the average of instantaneous differences of BP and BFV phases over the entire course of the chosen oscillation cycle(s) to provide statistically robust phase estimates.

2.5. *Transfer function analysis*

We also assessed cerebral autoregulation using a traditional Fourier-transform-based transfer function analysis [8, 35]. The time series BP and BFV were first linearly detrended and divided into 5000-point (100 s) segments with 50%

overlap. The Fourier transform of BP ($S_P(f)$) and BFV($S_V(f)$) were calculated for each segment with a spectral resolution 0.01 Hz, and were used to calculated the transfer function

$$H(f) = \frac{S_P(f)S_V^*(f)}{|S_P(f)|^2} = G(f)e^{i\phi(f)} \tag{5}$$

where $S_V^*(f)$ is the conjugate of $S_V(f)$; $|S_P(f)|^2$ is the power spectrum density of BP; $G(f) = |H(f)|$ is the transfer function amplitude (gain); and $\phi(f)$is the transfer function phase at a specific frequency f. The amplitude and the phase of the transfer function reflect the linear amplitude and time relationship between the two signals. The reliability of these linear relationships can be evaluated by coherence that ranges from 0 to 1:

$$C(f) = \frac{|S_P(f)S_V^*(f)|^2}{|S_P(f)|^2|S_V(f)|^2}. \tag{6}$$

It has been proposed that a coherence value <0.5 indicates a nonlinear BP–BFV relationship and engagement of autoregulation [8,35]. The estimates of BP–BFV relationship based on transfer function become unreliable for coherence values approaching zero.

Average coherence, gain, and phase were calculated in the frequency range <0.07 Hz in which the cerebral autoregulation was assumed to be most effective [8,15]. Transfer function analysis was also performed in the same frequency range as the observed dominant spontaneous oscillations in BP and BFV for comparison with the MMPF results (Table 3).

2.6. Receiver operating characteristic analysis

To compare the performances of the MMPF and transfer function analyses, we used the receiver operating characteristic analysis [36] to study the sensitivity and specificity of each method in distinguishing control and diabetic subjects. Briefly, this method chooses a discrimination threshold for BP–BFV phase shifts, and assigns subjects to the "diabetic" group (above the chosen threshold) or to the "control" group (below the chosen threshold) based on subjects' BP–BFV phase shifts. The sensitivity is the percentage of diabetic subjects correctly identified using the above criteria; and the specificity is the percentage of control subjects correctly identified. By choosing different values of the discrimination threshold, the sensitivity as the function of the specificity can be obtained. The plot of sensitivity vs. 1-specificity (receiver operating characteristic curve) is usually used to illustrate the performance of a method, and the area under the curve is a simple parameter to quantify the performance (Fig. 3). If the sensitivity is always equal to the specificity (the area under the curve = 0.5), then the method cannot distinguish control and diabetic subjects at all and thus has the worst performance. If the area value >0.5 and closer to 1.0, it will indicate a better discriminator between the control and diabetes groups and the method has a better performance.

3. Results

3.1. Mean values

We found no significant differences between the control and diabetic groups in age, body mass index, heart rate, and BP. The respiration frequency was higher and CO_2 lower in the diabetic group (Table 1). Cerebrovascular resistances were higher in the diabetic group (left side: $p = 0.04$; right side: $p = 0.06$). The average value of mean BFV was smaller in the diabetic group for both left and right sides, but only the group difference for the left side reached significant level (left: $p = 0.04$; right: $p = 0.06$) (Table 2).

3.2. MMPF results

3.2.1. BP–BFV phase shift in healthy subjects

For all healthy subjects, we found dominant oscillations in BP and BFV signals in the frequency range from 5 to 24 cycles/min (from 0.07 to 0.38 Hz: mean ± SE, 0.156 ± 0.015 Hz). These dominant oscillations correspond to the spontaneous and respiratory fluctuations in BP and BFV, and continuously modulate BP and BFV signals throughout the entire baseline. Panels 1–3 in Fig. 1A illustrate spontaneous oscillations in BP and right and left BFV signals for

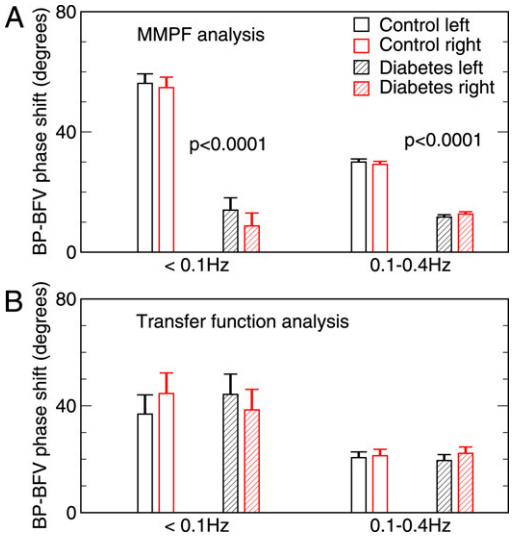

Fig. 2. Phase shifts between spontaneous blood pressure and blood flow oscillations in a low frequency band (<0.1 Hz) and in a high frequency band (0.1–0.4 Hz). (A) The MMPF results showed that BP–BFV phase shifts in diabetes were significantly smaller than those of controls in both frequency bands ($p < 0.0001$). (B) BP–BFV phase shifts obtained from the transfer function analysis showed no difference between control and diabetes in both low and high frequency bands.

Table 2
Cerebral blood flow measurements during baseline

Group	Control	Diabetes	P
Left systolic flow velocity (cm/s)	79.0 ± 4.1	65.8 ± 3.4	0.007
Left diastolic flow velocity (cm/s)	44.4 ± 2.7	33.8 ± 2.1	0.006
Left mean flow velocity (cm/s)	57.1 ± 2.9	46.2 ± 2.6	0.01
Left cerebrovascular resistance (mmHg s/cm)	1.67 ± 0.11	2.06 ± 0.14	0.04
Right systolic flow velocity (cm/s)	74.1 ± 3.7	61.9 ± 3.6	0.03
Right diastolic flow velocity (cm/s)	40.0 ± 2.4	34.3 ± 3.1	NS
Right mean flow velocity (cm/s)	54.6 ± 3.1	45.5 ± 3.2	NS
Right cerebrovascular resistance (mmHg s/cm)	1.76 ± 0.11	2.18 ± 0.18	NS

Data are presented as mean±SE. P values are for group comparison.

a healthy subject. The phase shifts between BFV and BP can be visualized in extracted dominant oscillations; i.e., the peak-valley positions of BFV were advanced than those of BP (Fig. 1A, panel 4). Instantaneous BP–BFV phase shifts, calculated by the Hilbert transform, varied over time (Fig. 1A, panel 5, solid lines). The averages of the instantaneous phase shifts between BFV and BP (Fig. 1A, panel 5, dashed lines) were positive in all 20 healthy subjects (left side: 37.3 ± 2.4 deg; right side: 38.0 ± 2.8 deg, mean ± SE), indicating that the BFV fluctuations precede fluctuations in peripheral BP. The BP–BFV phase shifts of left and right sides were highly correlated ($R^2 = 0.62$, $p < 0.0001$), indicating no side difference.

We also performed the MMPF analysis in two different frequency ranges: slower frequency range <0.1 Hz that is traditionally used for assessment of cerebral autoregulation, and faster frequency range 0.1–0.4 Hz to determine the effects of frequency of spontaneous oscillations on BP and BFV phase shift. Individual BP and BFV oscillatory cycles corresponding to each frequency range were selected. At the frequencies <0.1 Hz, BP–BFV phase shifts were 56.2 ± 4.0 deg (mean±SE) for the left side and 54.8 ± 4.3 deg for the right side (Fig. 2A). These results were similar to those observed during the Valsalva manoeuvre, in which BP/BFV oscillations are in the same frequency band (<0.1 Hz) [17]. At the frequency between 0.1 and 0.4 Hz, BP–BFV phase shifts were 30.0 ± 1.0 deg (mean ± SE) for left side and 29.2 ± 1.0deg for right side (Fig. 2A). These BP–BFV phase shifts were smaller than those at the frequency <0.1 Hz (Fig. 2A), and were close to the values obtained from dominant BP and BFV oscillations (Fig. 1C).

Table 3
Transfer function results

Group	0.01–0.07 Hz			0.1–0.4 Hz		
	Control ($n = 20$)	Diabetes ($n = 20$)	p	Control ($n = 20$)	Diabetes ($n = 20$)	P
Coherence (left)	0.47 ± 0.03	0.54 ± 0.3	NS	0.71 ± 0.03	0.60 ± 0.04	0.05
Coherence (right)	0.45 ± 0.02	0.50 ± 0.4	NS	0.70 ± 0.03	0.58 ± 0.4	0.02
Gain (left)	0.67 ± 0.09	0.67 ± 0.09	NS	1.07 ± 0.06	0.68 ± 0.08	0.0003
Gain (right)	0.65 ± 0.10	0.59 ± 0.08	NS	1.01 ± 0.07	0.63 ± 0.08	0.0006
Phase (left)	36.9 ± 7.2	44.3 ± 7.3	NS	20.6 ± 2.0	19.5 ± 2.3	NS
Phase (right)	44.6 ± 6.7	38.5 ± 8.8	NS	21.3 ± 2.6	22.2 ± 2.1	NS

Data are presented as mean ± SE. P values indicate between group comparisons.

3.2.2. *Effects of diabetes on BP–BFV phase shift*

For the 20 diabetic subjects, we also identified dominant and continuous spontaneous oscillations in BP and BFV during baseline in the frequency range from 0.15–0.38 Hz (mean ± SE: 0.25 ± 0.02 Hz) (Fig. 1B, panels 1–3). The phase shifts between BFV and BP oscillations in diabetic subjects were also positive (Fig. 1B panels 4–5) (mean±SE: left side, 14.9 ± 2.5 deg; right side, 15.6 ± 2.8 deg), but values were much smaller compared to the control group for both sides ($p < 0.0001$) (Fig. 1C). Considering the variations in the frequency of spontaneous oscillations among subjects and between the groups, we also analysed the BP–BFV phase shifts adjusted for the dominant frequency in MANOVA. This approach enabled us to identify the effects of diabetes on the BP–BFV relationship that were independent of the frequency of spontaneous oscillations. The frequency-adjusted BP–BFV shifts were also reduced in the diabetic group ($p < 0.001$) compared to the control group. This result is consistent with the results obtained by one-way analysis of variance between groups (Fig. 1C).

The reduction BP–BFV phase shifts in the diabetes group was also confirmed by analyzing BP and BFV oscillations in separate two frequency bands (<0.1 Hz and 0.1–0.4 Hz). At the frequency <0.1 Hz, BP–BFV phase shifts in diabetes (left side: 14.0 ± 4.1 deg; right side: 8.7 ± 4.3 deg) were smaller compared to the control group (left side: 56.2 ± 4.0 deg; right side: 54.8 ± 4.3 deg; $p < 0.0001$) (Fig. 2A). Similarly, in the frequency range 0.1- 0.4 Hz, BP–BFV phase shifts were smaller ($p < 0.0001$) in the diabetes (left side: 11.7 ± 0.8 deg; right side: 12.7 ± 0.8 deg) than in the control group (left side: 30.0 ± 1.0 deg; right side: 29.2 ± 1.0 deg) (Fig. 2A), which is the same frequency range of dominant BP and BFV oscillations for the diabetes group.

3.2.3. *Other influences on BP–BFV phase shift*

Within the diabetic group, no difference in the phase shifts was observed in the six hypertensive diabetic subjects (left side: 16.2 ± 5.6 deg, $p = 0.68$; right side: 20.9 ± 4.9 deg, $p = 0.20$) or in the six diabetic subjects with retinopathy (left: 13.2 ± 4.0 deg, $p = 0.97$; right: 17.7 ± 13.2 deg, $p = 0.52$) compared to other diabetic subjects. Within the diabetic group, six subjects with retinopathy had longer diabetes duration compared to other diabetic subjects without retinopathy ($p < 0.003$). The 10 diabetic subjects with autonomic neuropathy (2 with orthostatic hypotension) had the similar BP–BFV phase shifts as other diabetic subjects ($p > 0.4$). We did not find significant effects of age, sex, mean BP, baseline CO_2, hypertension, retinopathy, and side (left vs. right). In addition, we did not find dependence of the BP–BFV phase shifts on BFV ($R^2 < 0.001$, $p > 0.5$) or cerebrovascular resistances ($R^2 < 0.02$, $p > 0.5$) for both left and right sides. Effects of hemoglobin A1C, diabetes duration, and glucose within diabetic group could not be reliably identified due to the sample size.

3.3. *Transfer function coherence, gain and phases*

Transfer function analysis of BP and BFV signals did not reveal significant differences between control and diabetic subjects in coherence, transfer function gains and phases over the frequency range <0.1 Hz (Table 3 and Fig. 2B). In the frequency between 0.1 and 0.4 Hz, diabetic subjects had lower coherence and lower gain than control subjects for both left and right sides (Table 3) but transfer function phase was not different between the two groups.

3.4. *Receiver operating characteristic analysis*

The receiver operating characteristic analysis showed that the area under the sensitivity-specificity curve for MMFP-based phase shifts (left side: 0.94 ± 0.04; right side: 0.87 ± 0.06) is larger than those of transfer function

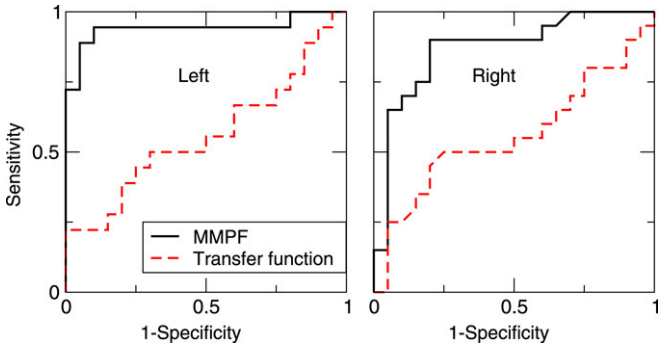

Fig. 3. Receiver operating characteristic curves for the diabetes prediction using blood pressure–blood flow velocity (BP–BFV) phase shifts obtained from the multimodal pressure flow method (MMPF) and using transfer function phases (0.1–0.4 Hz). The y axis is the sensitivity, representing the percentage of diabetes subjects identified; and the x axis is the 1-specificity; i.e., the percentage of control subjects that are incorrectly identified as diabetes subjects. The areas under the curves closer to 1.0 for BP–BFV phase shifts indicates that the MMPF measure serves as a better discriminator between the control and diabetes subjects than traditional transfer function analysis.

phases (left side: 0.56 ± 0.09, $p < 0.001$; right side: 0.56 ± 0.09, $p = 0.003$) (Fig. 3), indicating the MMPF measures may serve as a more sensitive biomarker for the diabetes prediction than the traditional transfer function phase.

4. Discussion

4.1. Assessment of nonlinear interactions between nonstationary signals

A major problem in contemporary physiology is the presence of nonstationarities in time series (statistical properties such as mean and standard deviation vary with time). Nonstationarity is an intrinsic feature of physiological data in both healthy and pathologic conditions, and are present even without external stimulation [37–39]. Since traditional analyses are often based on theories that assume stationary time series, various problems related to nonstationarity are encountered when attempting to extract both static and dynamic properties of physiological data [40,41]. Therefore, quantification of nonlinear interactions between two nonstationary signals presents a computational challenge. To resolve the difficulties related to nonstationary behaviour in physiological signals, investigators have applied concepts and methods derived from statistical physics and nonlinear dynamics [17,42–48]. For example, phase synchronization technique that was used for the assessment of coupling between chaotic oscillators in physical systems has been modified and applied to study interactions among physiological systems including cardiovascular system, respiration, locomotor activity, and neuronal activity in brain [45,46,48,49]. These studies have shown that nonlinear approaches can provide new information about the control mechanisms of physiological systems that may be difficult to be characterized using traditional approaches. Despite of progress, methods to reliably quantify nonlinear interactions between nonstationary signals are still lacking.

We aimed to tackle the important generic problem related to nonstationarity by designing and improving physics approaches to explore nonlinear interactions between peripheral blood pressure and blood flow velocity in cerebral arteries. In this study we proposed an improved MMPF method to study the nonlinear BP–BFV phase relationship in healthy and diabetic subjects during supine resting conditions, that is derived from our previous studies [17,48]. Unlike the traditional Fourier transform-based approaches, we did not assume BP and BFV as superimposed sinusoidal oscillations of constant amplitude and period in a preset frequency range. The new analysis uses an adaptive signal processing algorithm, Ensemble Empirical Mode Decomposition, to extract spontaneous oscillations that are actually embedded in BP and BFV fluctuations. We showed that the phases of spontaneous BFV oscillations were advanced compared to the phases of BP oscillations; i.e., flow oscillations preceded systemic pressure oscillations (Figs. 1 and 2). The BP–BFV phase shifts were similar to those observed during the Valsalva manoeuvre obtained from the MMPF method [17]. Such positive phase shift has been also reported using Fourier transform methods during head-up tilt, and was interpreted as a faster recovery of BFV mediated by the compensatory cerebral autoregulatory mechanisms [8,12,14,50]. Our previous studies showed that the reduction of the MMPF derived BP–BFV phase shifts was associated with impaired cerebral autoregulation in stroke and hypertensive subjects and in patients with traumatic brain injuries

[17,51], indicating that MMPF results reflect dynamics of cerebral autoregulation. Here we showed that BP–BFV phase shifts in diabetic subjects were significantly reduced and closer to zero, resembling that in patients with stroke or traumatic brain injuries [17,51]. This finding indicates that diabetes is also associated with impairment of dynamical cerebral autoregulation. At the same time, the phase shift calculated using the univariate transfer function analysis did not reveal any significant group differences. Consistently we found that the MMPF had a better performance in discriminating between control subjects and subjects with type 2 diabetes mellitus (Fig. 3). The different results obtained from the two analyses may be not surprising, considering the fact that the BP–BFV phase shifts of transfer function analysis are based on the Fourier transform which has limited application for nonstationary BP and BFV signals and nonlinear BP–BFV relationships. Note that our proposed method is not only applicable for the study of interactions between BP and BFV. Instead the method and its concepts can be potentially used to explore nonlinear interactions in other physical and physiological systems.

4.2. Active frequency range of cerebral autoregulation

It has been proposed that cerebral autoregulatory mechanisms act as a high-pass filter-cybernetic model [8,13], being more active at lower frequencies (<0.1 Hz) and less effective for faster spontaneous fluctuations at respiration frequency. This model predicts that, for a normal cerebral autoregulation, a *very* slow oscillation in BP (frequency approaching zero) will generate an oscillation in BFV with very small amplitude and an advanced phase close to 90 deg while a fast oscillation in BP will be completely transmitted to a BFV oscillation with phase lag close to zero. Though there is no established physiological neural pathway that can account for the high-pass filter mechanism, the frequency dependent influence of cerebral autoregulation was supported by many studies that are based on the transfer function analysis [10,11,15,52]. For instance, it has been shown that average amplitude (gain) of transfer function of BP and BFV was smaller at <0.07 Hz than at >0.07 Hz, phase had a maximum (∼60 deg) at ∼0.05 Hz, and coherence of BP–BFV transfer function was close to 1.0 at frequency >0.07 Hz and was smaller (∼0.5) at frequencies <0.07 Hz. The small coherence at lower frequencies indicates the absence of linear BP–BFV relationship, and was interpreted as the effect of cerebral autoregulation [10].

It is important to note that coherence, gain, and phase of transfer function are continuous functions of frequency and do not exhibit apparent transition points at a specific frequency. Thus, the model and transfer function results do not necessarily indicate that cerebral autoregulation is active and has influence on blood flow regulation only in certain frequency region. Although many studies selected frequency <0.1 Hz in the transfer function analysis, such choice of frequency range for the estimation of cerebral autoregulation is somewhat arbitrary. Previous studies showed that after a sudden blood flow decline, baseline levels can be restored within 3–6 s (corresponding to 0.16–0.33 Hz in frequency domain) [53,54]. Therefore, there is no reason to refute the notion that cerebral autoregulation can operate at frequencies >0.1 Hz. Studies of using phase synchronization technique and transfer function analysis also indicated that the relationship between BP and BFV oscillations at frequency >0.1 is altered in patients with strokes and, thus, may also provide useful information on cerebral autoregulation [48,55]. In patients with abnormal autoregulation after a traumatic brain injury BP–BFV phase shift in the frequency range of 0.1–0.3 Hz was around 10 deg (left side 10.2 ± 9.5 deg; right side 11.6 ± 13.3 deg) [51]. Thus, our findings that BP–BFV phase shifts are larger in controls in the frequency range (0.1–0.4 Hz) supports the notion that cerebral autoregulation may influence pressure-flow relationship at the frequency >0.1 Hz, as well as at the frequency <0.1 Hz.

Moreover, the transfer function analysis is based on Fourier transform that implicitly assumes stationary signals composed of sinusoidal oscillations of constant amplitude and period. During physiological recordings, BP and BFV signals are nonstationary and exhibit dynamic changes over time [56]; i.e., shifts of respiratory frequencies to slower range, occurrence of spontaneous waves, and etc. Therefore, a single transfer function may be not sensitive enough to identify the influences of cerebral autoregulation at different time scales and to assess nonlinearities in pressure-flow relationship using a small sample size of subjects. Furthermore, another intrinsic problem of the transfer function is that low values of univariate coherences between two signals (e.g., coherence <0.5 for BP–BFV transfer function at frequency <0.07 Hz) violate the assumption of a linear relationship between two signals and thus may preclude use of gain and phase as measures of coupling strength between BFV and BP [57].

In the present study, we demonstrated that the BP–BFV phase shifts in both low (<0.1 Hz) and higher frequency (∼0.1–0.4 Hz) bands may reflect cerebral autoregulation and that such phase shift was significantly reduced in diabetic subjects, indicating impaired autoregulation. These findings provide additional important evidence to support that

cerebral autoregulation is a continuous dynamic process, influencing BP–BFV relationship at multiple time-scales over a larger frequency range. They also suggest that inherent nonlinearities of cerebral autoregulation can be better described by nonlinear methods such as MMPF [17,48,51], multivariate coherence [57], and general Volterra–Wiener approaches [56,58,59].

4.3. Assessment of cerebral autoregulation from spontaneous BP/BFV oscillations

Cerebral autoregulation dynamics are usually evaluated by the changes in BFV and BP during the interventions that induce rapid BP reductions or increases such as the Valsalva maneuver, thigh cuff deflation and the head-up tilt [2,9,50, 60–63]. The conventional approach is valuable, because it allows assessments of the autoregulation responses during rapid variations in systemic pressure under the stressed conditions. These tests, however, require patient cooperation and cannot be administered in acute care settings. More importantly, autoregulation is a dynamic process that is always engaged to control blood flow redistribution in response to local perfusion and metabolic needs during increased neuronal activity as well as systemic demands. Spontaneous fluctuations in cerebral blood flow reflect coupling of cardiovascular and respiratory responses to these perturbations. Therefore, there is a critical need to assess dynamics of autoregulation during *spontaneous* BP and BFV fluctuations. This issue has been successfully addressed with the improved MMPF method.

4.4. Dominant spontaneous oscillations in BP and BFV fluctuations

One interesting finding in this study is that the improved decomposition method can reveal dominant oscillations embedded in spontaneous BP and BFV fluctuations at the frequency between 0.07 and 0.4 Hz. These dominant oscillations persist continuously in a certain intrinsic mode function for an individual during the entire baseline recordings. Since averaging over more oscillatory cycles can statistically provide more accurate estimates of BP–BFV phase shifts, the spontaneous continuous oscillations can potentially enable very reliable assessment of BP–BFV phase relationship. In addition, extracting these continuous oscillations in a certain decomposed mode function can be more objective than selecting an individual oscillatory cycle that involves more subjective human judgments. One concern is that the frequency of dominant BP and BFV oscillations during baseline conditions was between 0.07 and 0.4 Hz, which is traditionally believed to be out of active range of cerebral autoregulation. However, this study and recent studies [17,51] showed that impairment of cerebral autoregulation in type 2 diabetes, stroke, hypertension and brain injury have significant influences on the BP–BFV relationship at the higher frequency range (>0.1 Hz) (see Section 4.2). Encouraged by these findings, we believe that dominant spontaneous BP and BFV oscillations during resting conditions can be useful and even advantageous for noninvasive assessment of cerebral autoregulation. Further systematic studies are needed to identify the causes for the presence of dominant oscillations and to determine the frequency dependence of the BP–BFV phase shift.

4.5. Impairment of autoregulation in diabetes

Diabetes is a complex metabolic disease with significant effects on the systemic and cerebral vasculature [24], vasomotion and reduced cerebral blood flow and vasoreactivity to CO_2 [64]. With impairment of vasoregulation, spontaneous variations in systemic pressure during everyday activities may perturb cerebral perfusion pressure. Therefore, older diabetic patients may experience larger fluctuations of perfusion pressure that may have implications for cerebral hypoperfusion and brain atrophy [65,66]. Consistently, we found in this study that cerebral flow velocity in diabetes was more passively dependent on blood pressure, as indicated by reduced phase shifts between oscillations in the two physiological variables during resting conditions.

There are still many important questions on cerebral blood flow regulation in diabetes that could not be rigorously tested in our study groups due to the small sample size, including the effects of co-morbidities, duration of diabetes and its control, orthostatic hypotension, haemoglobin A1C, glucose levels, and other diabetes-related risk factors for cerebrovascular systems. Larger prospective studies are also needed to determine whether these factors affect dynamic indices of autoregulation and also whether MMPF-based indices of autoregulation have predictive value for late complications of diabetes.

5. Conclusions

In conclusion, our results indicate that the BP–BFV phase shift obtained by the improved MMPF method can be used to assess the nonlinear dynamics of the central blood flow-pressure relationship during supine baseline conditions. Instantaneous pressure-flow phase shift provides a sensitive and robust measure of impaired autoregulation in the diabetes group. The proposed method is robust, computationally feasible and has broad applications for quantification of the instantaneous phase relationship of nonlinear and nonstationary physiological signals.

Acknowledgements

This study was supported by an American Diabetes Association Grant 1-03-CR-23 and 1-06-CR-25, NIH-NINDS R01-NS045745 to V. Novak, NIH-NINDS STTR grant 1R41NS053128-01A2 to V. Novak in collaboration with DynaDx, Inc., a CIMIT New Concept Grant (W81XWH,) an NIH Older American Independence Center Grant 2P60 AG08812 and NIH Program Project AG004390 and a General Clinical Research Center (GCRC) Grant MO1-RR01302, and James S. McDonnell Foundation, the Ellison Medical Foundation Senior Scholar in Aging Award, the G. Harold and Leila Y. Mathers Charitable Foundation, Defense Advanced Research Projects Agency, and the NIH/National Center for Research Resources (P41RR013622). Norden E. Huang is supported in part by a Chair at NCU endowed by Taiwan Semiconductor Manufacturing Company, Ltd., and a grant, NSC 95-2119-M-008-031-MY3, from the National Research Council, Taiwan, ROC. Zhaohua Wu is supported by National Science Foundation of USA under grants ATM-0342104 and ATM-0653123. The authors acknowledge the contributions of Professor Ary Goldberger, MD.

References

[1] R. Aaslid, in: D.W. Newell, R. Aaslid (Eds.), Transcranial Doppler, Raven Press, New York, 1992, p. 49 (Chapter 5).
[2] R.B. Panerai, Physiol. Measurements 19 (1998) 305.
[3] S. Schwarz, D. Georgiadis, A. Aschoff, S. Schwab, Stroke 33 (2002) 497.
[4] P.J. Eames, et al., J. Neurol. Neurosurg. Psychiatry 72 (2002) 467.
[5] S.L. Dawson, R.B. Panerai, J.F. Potter, Cerebrovascular Dis. 16 (2003) 67.
[6] E.A. Schmidt, et al., J. Neurosurgery 99 (2003) 991.
[7] M. Czosnyka, et al., Neurosurgery 41 (1997) 11; discussion 17-9.
[8] R.R. Diehl, D. Linden, D. Lucke, P. Berlit, Stroke 26 (1995) 1801.
[9] B.J. Carey, R.B. Panerai, J.F. Potter, Stroke 34 (2003) 1871.
[10] C.A. Giller, Neurosurgery 27 (1990) 362.
[11] C.A. Giller, D.G. Iacopino, Neurological Res. 19 (1997) 634.
[12] A.A. Birch, et al., Stroke 26 (1995) 834.
[13] R.R. Diehl, D. Linden, D. Lucke, P. Berlit, Clin. Auton. Res. 8 (1998) 7.
[14] A.P. Blaber, et al., Stroke 28 (1997) 1686.
[15] R. Zhang, J.H. Zuckerman, C.A. Giller, B.D. Levine, Am. J. Physiol. 274 (1998) H233.
[16] C. Haubrich, et al., Acta Neurologica Scandinavica 109 (2004) 210.
[17] V. Novak, et al., BioMed. Eng. OnLine 3 (2004) 39.
[18] R.I. Kitney, T. Fulton, A.H. McDonald, D.A. Linkens, J. Biomed. Eng. 7 (1985) 217.
[19] V. Novak, et al., J. Appl. Physiol. 74 (1993) 617.
[20] R.R. Diehl, B. Diehl, M. Sitzer, M. Hennerici, Neurosci. Lett. 127 (1991) 5.
[21] J.M. Karemaker, in: P.A. Low (Ed.), Clinical Autonomic Disorders: Evaluation and Management, 2 ed., Lippincott-Raven Publishers, Philadelphia, 1997, p. 309.
[22] T.B. Kuo, et al., J. Cerebral Blood Flow & Metabolism 18 (1998) 311.
[23] Z. Wu, N.E. Huang, Centre for ocean-land-atmosphere studies, Tech. Rep. No. 193, 2005.
[24] T.A. Baird, et al., J. Clin. Neurosci. 9 (2002) 618.
[25] P. Dandona, et al., Br. Med. J. 29 (1978) 325.
[26] D.N. Griffith, et al., Diabet. Med. 4 (1987) 217.
[27] B. Zvan, et al., Cerebrovasc Dis. 15 (2003) 270.
[28] L.M. Aiello, J.D. Cavallerano, A.A. Cavallerano, S.E. Bursell, Ophtalmolol Clin. North. Am. 13 (2000) 213.
[29] A.A. Cavallerano, et al., Retina 23 (2003) 215.
[30] P.A. Low, Current Opinion Neurol. Neurosurgery 5 (1992) 461.
[31] W. Huang, Z. Shen, N.E. Huang, Y.C. Fung, Proc. Natl. Acad. Sci. USA 95 (1998) 4816.
[32] N.E. Huang, et al., Proc. Roy. Soc. London A454 (1998) 903.
[33] D. Gabor, J IEE (London) 93 (III) (1946) 429.

[34] A.V. Oppenheim, R.W. Schafer, J.R. Buck, Discrete-Time Signal Processing, 2nd ed., Prentice-Hall, Inc., 1999.
[35] L.A. Lipsitz, et al., Stroke 31 (2000) 1897.
[36] M.H. Zweig, G. Campbell, Clin. Chem. 39 (1993) 561.
[37] H. Kantz, T. Schreiber, Nonlinear Time Series Analysis, Cambridge University Press, Cambridge, 1997.
[38] G.M. Viswanathan, C.K. Peng, H.E. Stanley, A.L. Goldberger, Phys. Rev. E. Stat. Phys. Plasmas. Fluids Relat. Interdiscip. Topics. 55 (1997) 845.
[39] P. Bernaola-Galvan, P.C. Ivanov, L.A. Nunes Amaral, H.E. Stanley, Phys. Rev. Lett. 87 (2001) 168105.
[40] K. Hu, et al., Phys. Rev. E Stat. Nonlin. Soft. Matter Phys. 64 (2001) 011114.
[41] Z. Chen, P.C. Ivanov, K. Hu, H.E. Stanley, Phys. Rev. E Stat. Nonlin. Soft. Matter Phys. 65 (2002) 041107.
[42] J.J. Collins, I.N. Stewart, J. Math. Biol. 30 (1992) 827.
[43] C.K. Peng, et al., Phys. Rev. Lett. 70 (1993) 1343.
[44] J.J. Collins, C.J. De Luca, Phys. Rev. Lett. 73 (1994) 764.
[45] P. Tass, et al., Phys. Rev. Lett. 81 (1998) 3291.
[46] C. Schafer, M.G. Rosenblum, H.H. Abel, J. Kurths, Phys. Rev. E. Stat. Phys. Plasmas. Fluids Relat. Interdiscip. Topics. 60 (1999) 857.
[47] M. Costa, A.L. Goldberger, C.K. Peng, Comput. Cardiol. 29 (2002) 137.
[48] Z. Chen, et al., Phys. Rev. E. Stat. Nonlin. Soft. Matter Phys. 73 (2006) 031915.
[49] D.M. Bramble, D.R. Carrier, Science 219 (1983) 251.
[50] R.B. Panerai, S.L. Dawson, P.J. Eames, J.F. Potter, Am. J. Physiol. 280 (2001) H2162–H2174.
[51] K. Hu, et al. Cardiovascular Eng. (2007), in press (doi:10.1007/s10558-007-9045-5).
[52] J.W. Hamner, et al., J. Physiol. 559 (2004) 965.
[53] L. Symon, K. Held, N.W. Dorsch, Stroke 4 (1973) 139.
[54] R. Aaslid, K.F. Lindegaard, W. Sorteberg, H. Nornes, Stroke 20 (1989) 45.
[55] R.B. Panerai, J.M. Rennie, A.W. Kelsall, D.H. Evans, Med. Biol. Eng. Comput. 36 (1998) 315.
[56] G.D. Mitsis, M.J. Poulin, P.A. Robbins, V.Z. Marmarelis, IEEE Trans. Biomed. Eng. 51 (2004) 1932.
[57] R.B. Panerai, P.J. Eames, J.F. Potter, Am. J. Physiol. Heart Circ. Physiol. 291 (2006) H251–H259.
[58] G.D. Mitsis, R. Zhang, B.D. Levine, V.Z. Marmarelis, J. Appl. Physiol. 101 (2006) 354.
[59] G.D. Mitsis, R. Zhang, B.D. Levine, V.Z. Marmarelis, Ann. Biomed. Eng. 30 (2002) 555.
[60] V. Novak, et al., Stroke 29 (1998) 1876.
[61] F.P. Tiecks, A.M. Lam, R. Aaslid, D.W. Newell, Stroke 26 (1999) 1014.
[62] S.L. Dawson, R.B. Panerai, J.F. Potter, J. Appl. Physiol. 86 (1999) 675.
[63] V. Novak, et al., Neurology 60 (2003) 1657.
[64] V. Novak, et al., Diabetes Care 29 (2006) 1529.
[65] D. Last, et al., Diabetes Care (2007).
[66] S.M. Manschot, et al., Diabetes 55 (2006) 1106.